Supplementary Figures for Manuscript

Activation of PKA leads to mesenchymal-to-epithelial transition and loss of tumor-initiating ability

Diwakar R. Pattabiraman[1], Brian Bierie[1], Katharina Isabelle Kober[1], Prat Thiru[1], Jordan Krall[1], Christina Zill[1], Ferenc Reinhardt[1], Wai Leong Tam[1,4,5] and Robert A. Weinberg[1,2,3*]

Supplementary Figure 1:

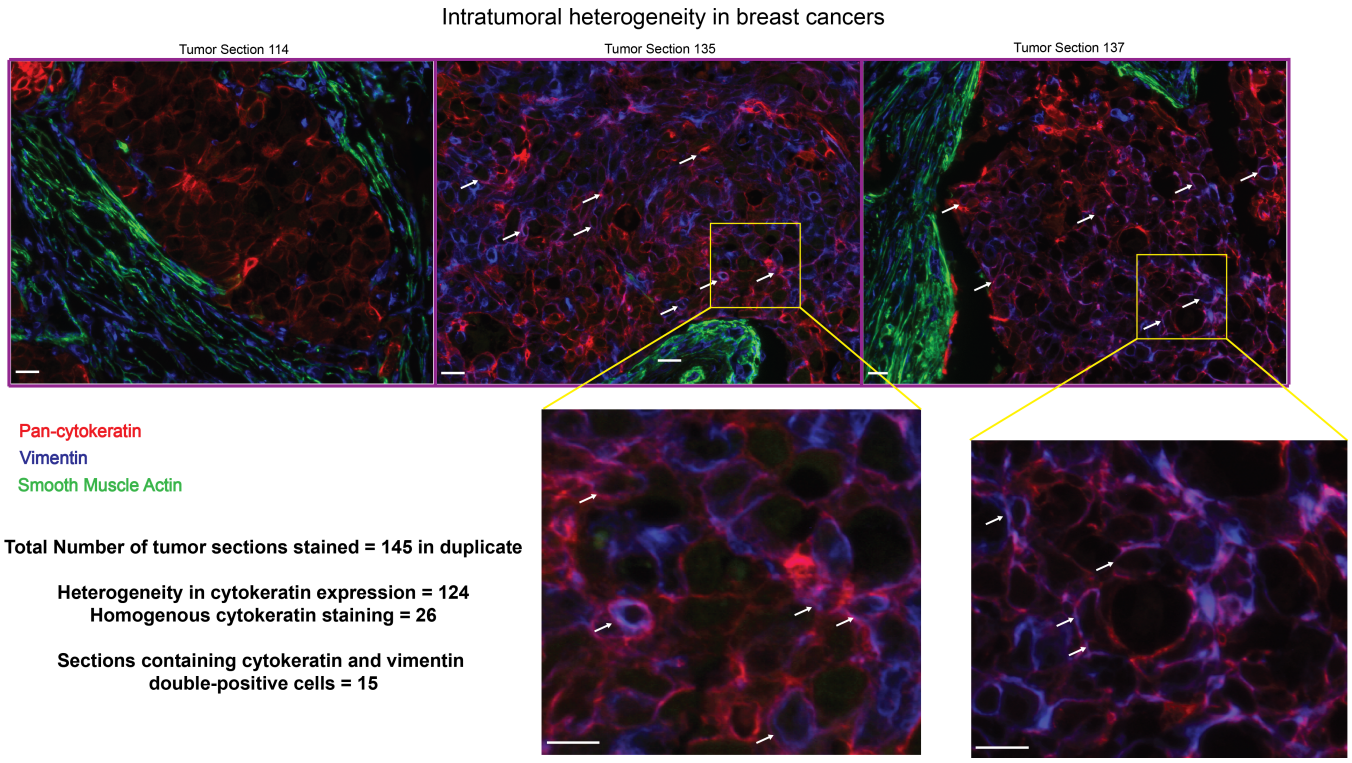

Figure S1: Breast cancers contain high levels of intratumoral heterogeneity containing a mixture of epithelial and mesenchymal characteristics: Immunofluorescence of tissue microarrays containing 145 breast cancers show that a majority of breast cancers express heterogeneous levels of cytokeratins with magnified sections showing co-staining of cytokeratin and vimentin indicating cells of mixed epithelio-mesenchymal nature, indicated by white arrows. Legend: Red – Pan-cytokeratin, Blue – Vimentin, Green – Smooth muscle actin. All scale bars - 25μm

Supplementary Figure 2:

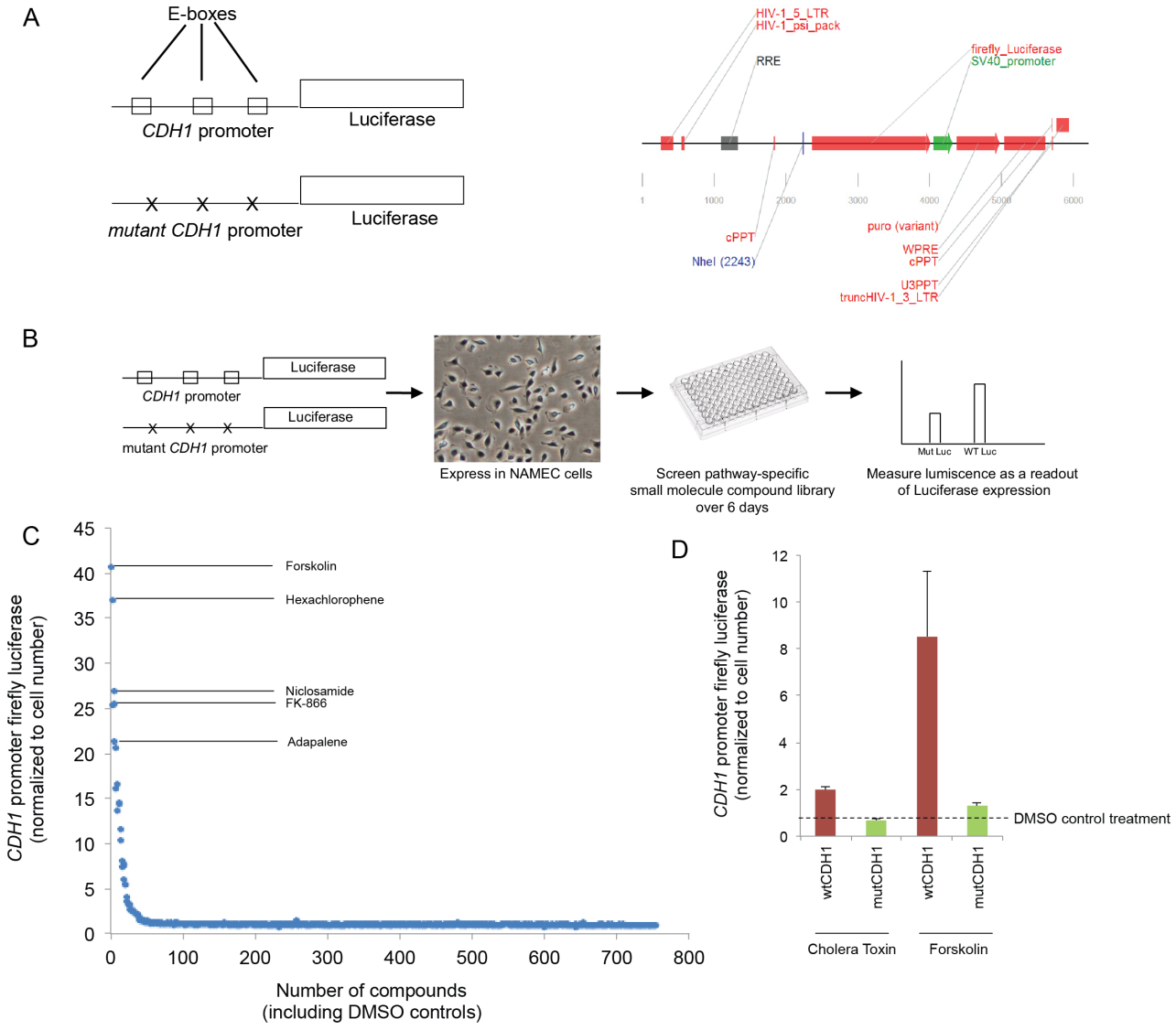

Figure S2: Screen to identify regulators of *CDH1* in mesenchymal mammary epithelial cells. (A) The screen was performed with a reporter containing a section of the *CDH1* promoter containing three E-boxes. The screen was performed as shown in (B) over 6 days with a number of hits that were able to activate the reporter (C). *CDH1* promoter luciferase values are normalized to CellTiter Glo values, and data is presented relative to DMSO control treatment. Compounds that resulted in excessive cell death (CTG value < 6000) were excluded from the plot. Independent validation of the screen showed an activation of the *CDH1* reporter upon treatment of N8 cells with forskolin and CTx (D).

Supplementary Figure 3:

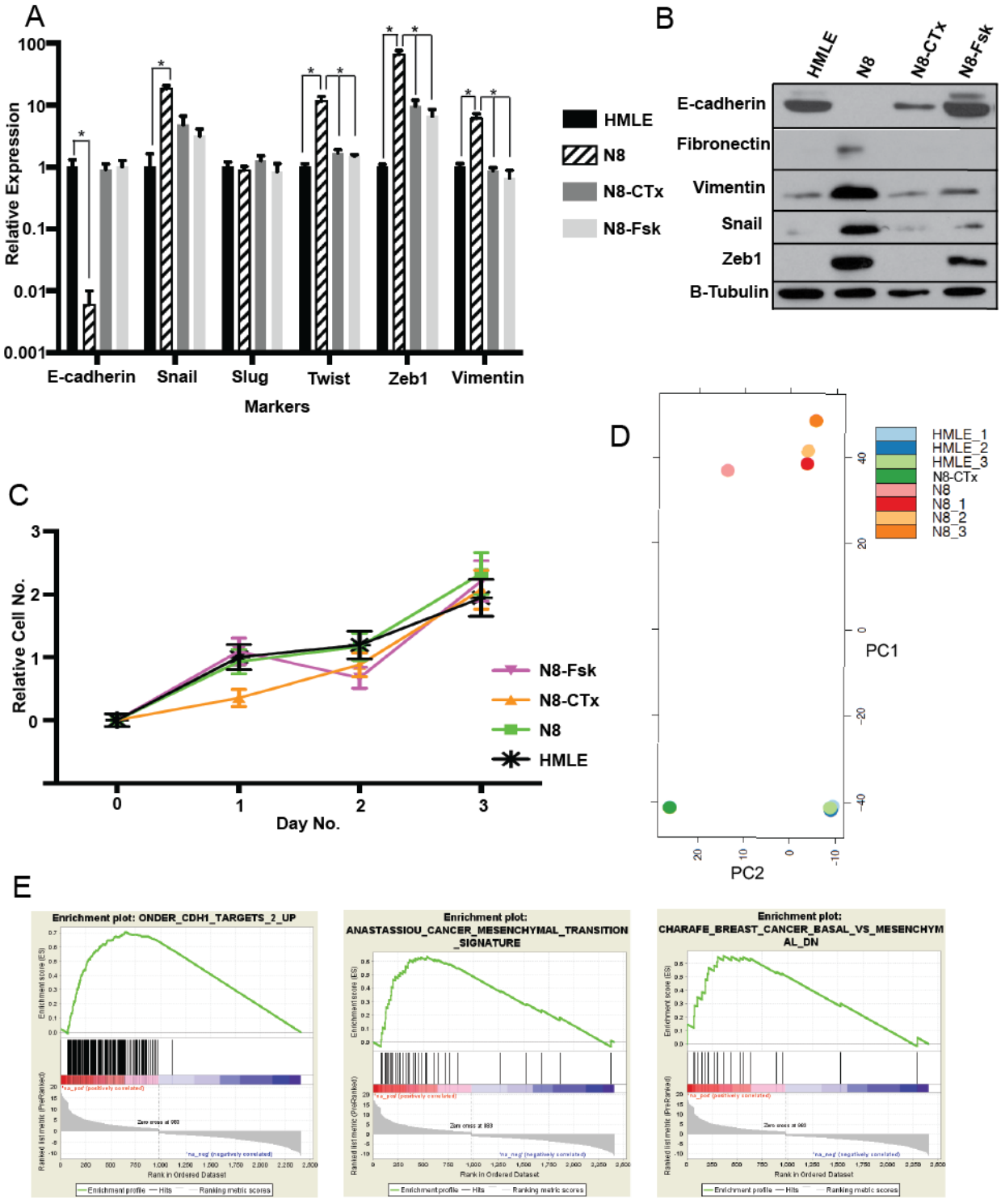

Figure S3: Properties of cells that have undergone a mesenchymal-to-epithelial transition. Cells that have undergone an MET upon treatment with CTx or Fsk undergone gene expression changes of epithelial and mesenchymal markers (A) (mean ± SD, $p<0.05$, n=3; Student t-test) as well as changes in protein expression (B) indicating a *bona fide* transition to the epithelial state. CyQuant assays (C) were performed to assess the effect of CTx and Fsk on the rate of proliferation of the cells (mean ± SD, n=3). (D) Principal component analysis of RNA-Seq data comparing HMLE and N8 cells to N8-CTx cells that have undergone an MET. (E) Gene set enrichment analysis show that the gene expression changes during the transition between the N8 and N8-CTx state are reminiscent of an EMT signature.

Supplementary Figure 4:

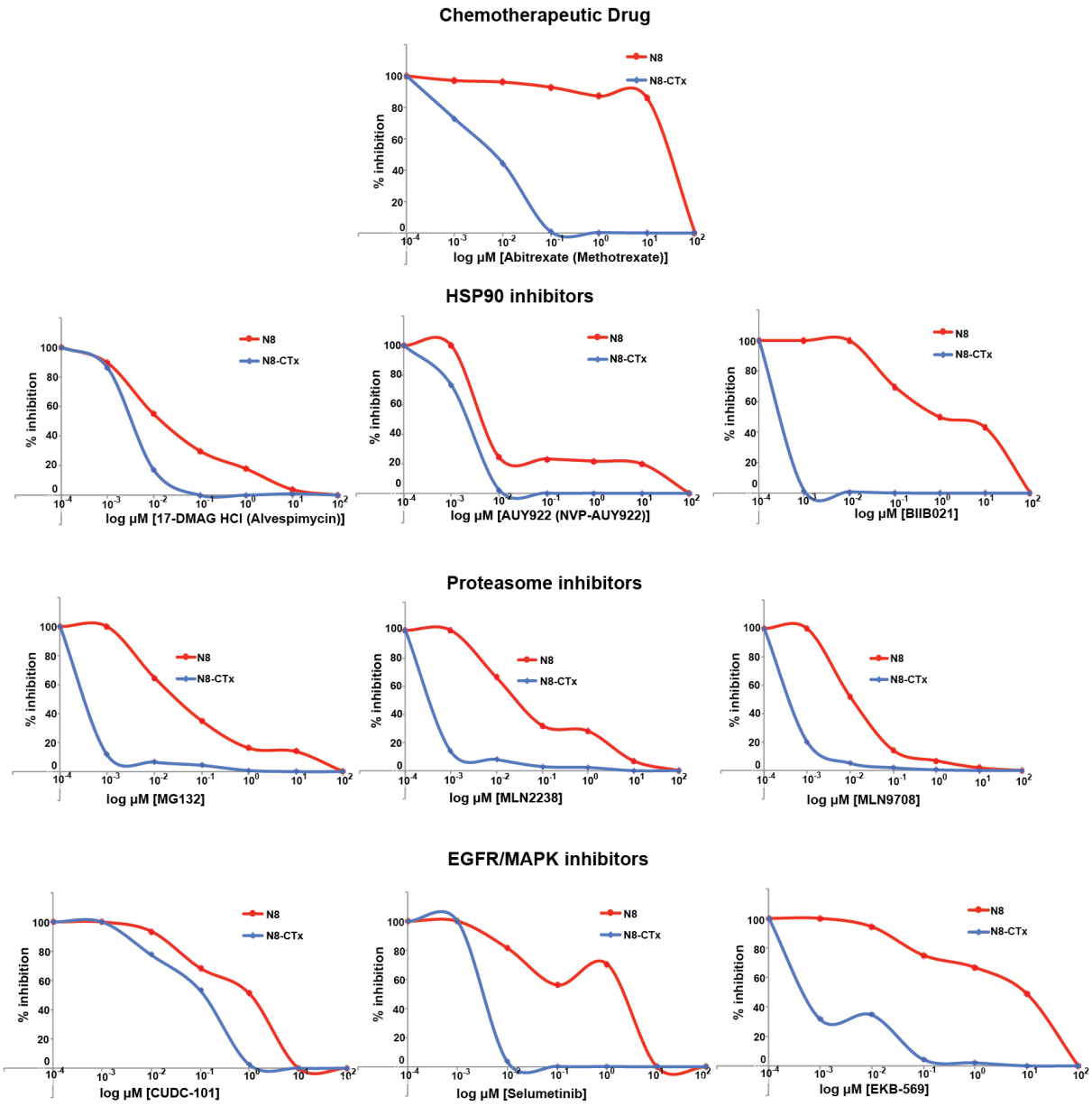

Figure S4: Cells that have undergone an MET are more susceptible to a range of drugs and inhibitors. N8 and N8-CTx cells were screened against the Selleck anti-cancer compound library and the Enzo Kinase Inhibitor Library to compare their sensitivities to a range of different chemotherapeutic compounds as well as inhibitors of various cancer-related pathways. As seen from the screen, the N8-CTx cells are more sensitive to chemotherapeutic drugs such as methotrexate, HSP90 inhibitors, proteasome inhibitors and EGFR/MAPK pathway inhibitors.

Supplementary Figure 5:

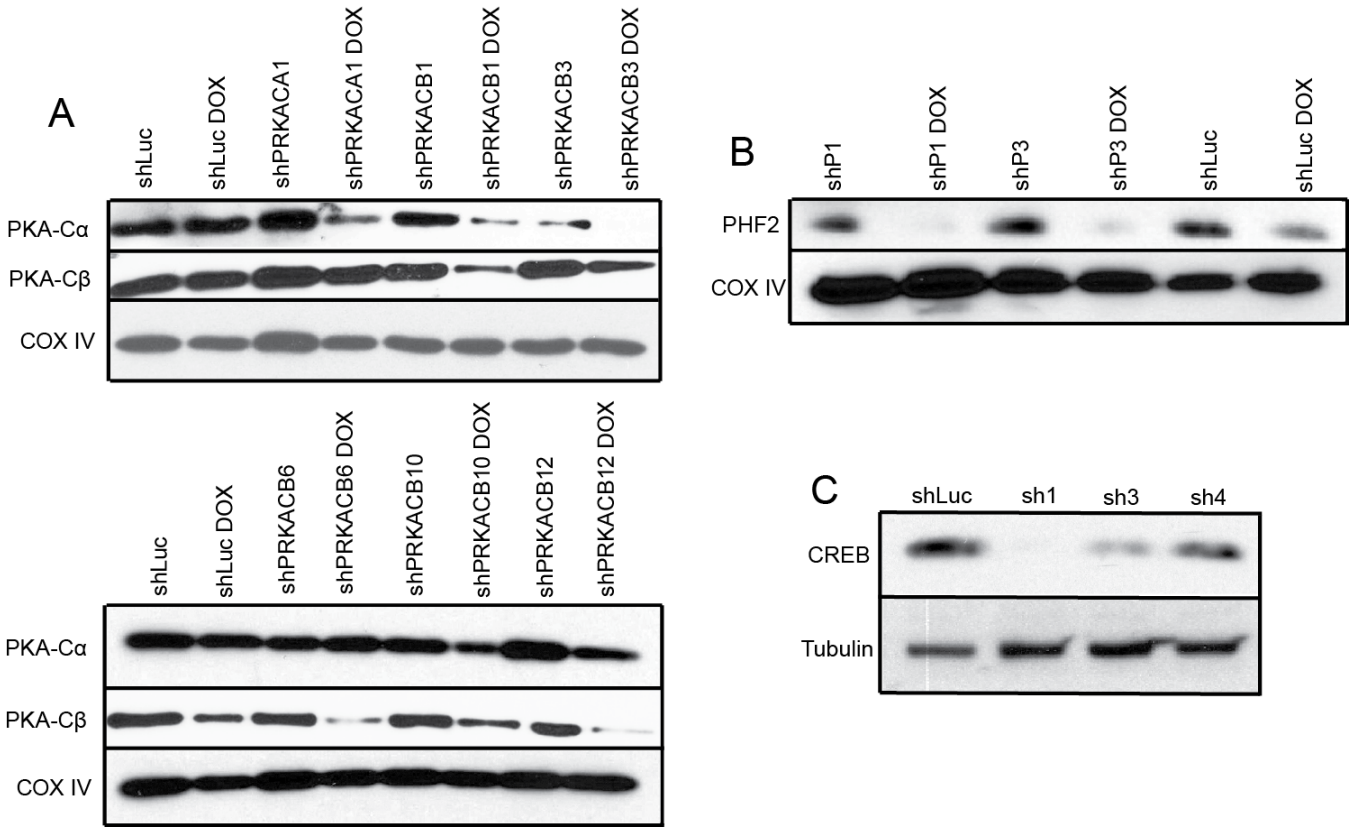

Figure S5: shRNA-mediated knockdown of PKA, PHF2 and CREB1 levels. Loss of function of PKA and PHF2 was assayed by cloning shRNAs into the Tet-pLKO-puro vector. The ability of various hairpins to knockdown expression levels of (A) PKA, (B) PHF2 and (C) CREB1 was measured by western blotting.

Supplementary Figure 6:

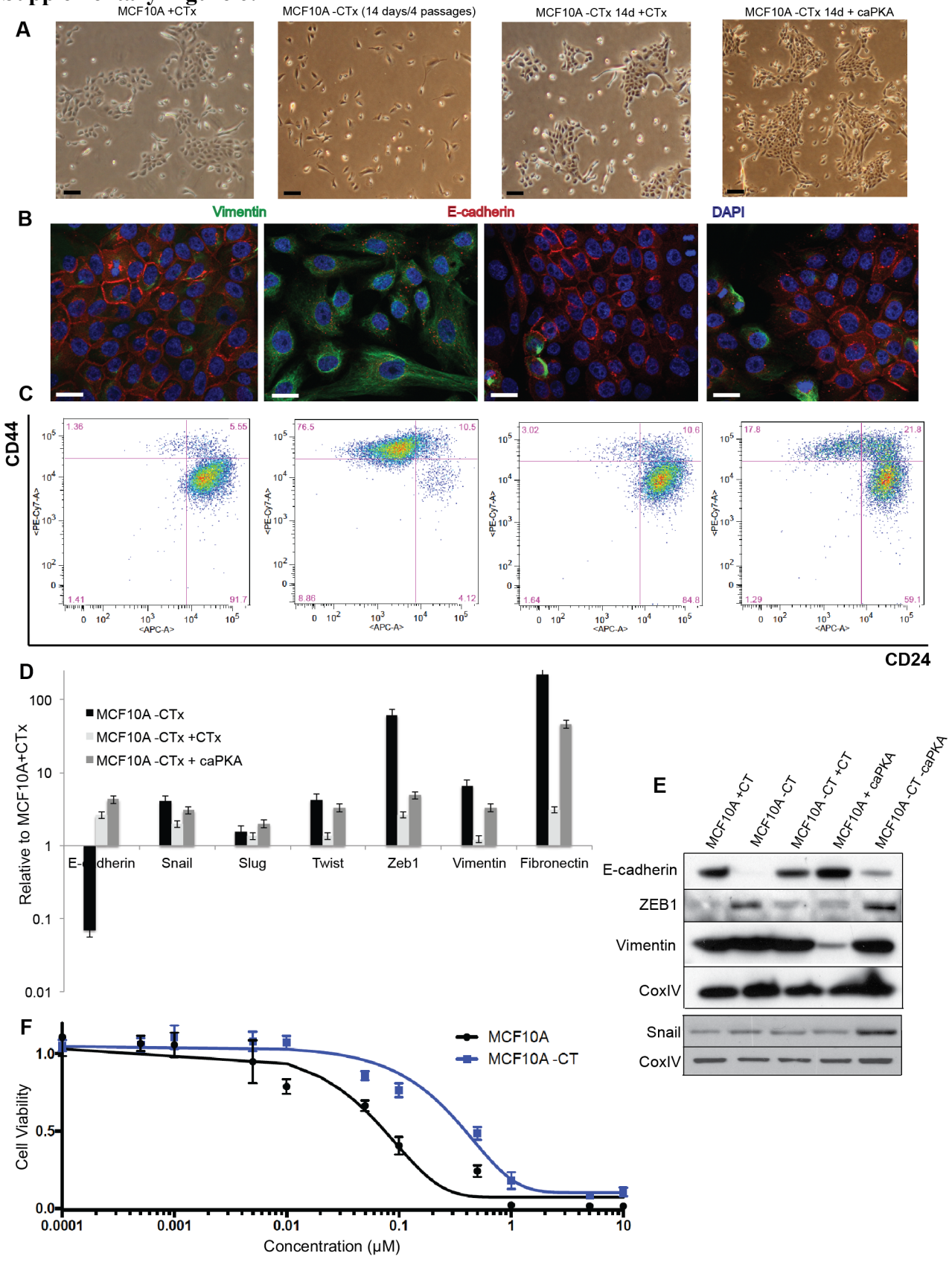

Figure S6: MCF10A cells undergo an EMT in the absence of CTx. MCF10A cells that are normally cultured in the presence of CTx were grown in its absence for 2 weeks, following which CTx was re-added or an active mutant of PKA was ectopically expressed. In both cases, the cells re-acquired epithelial properties as observed by (A) changes in morphology, (B) immunofluorescence for E-cadherin and Vimentin, (C) FACS to assess the CD44 CD24 status of the cells and estimating the expression levels of epithelial and mesenchymal markers by (D) qRT-PCR (mean ± SD, n=3) and (E) western blotting. Cells that are mesenchymal following withdrawal of CTx are more resistant to treatment with doxorubicin (F) (mean ± SD, n=4). All scale bars - 25μm.

Supplementary Figure 7:

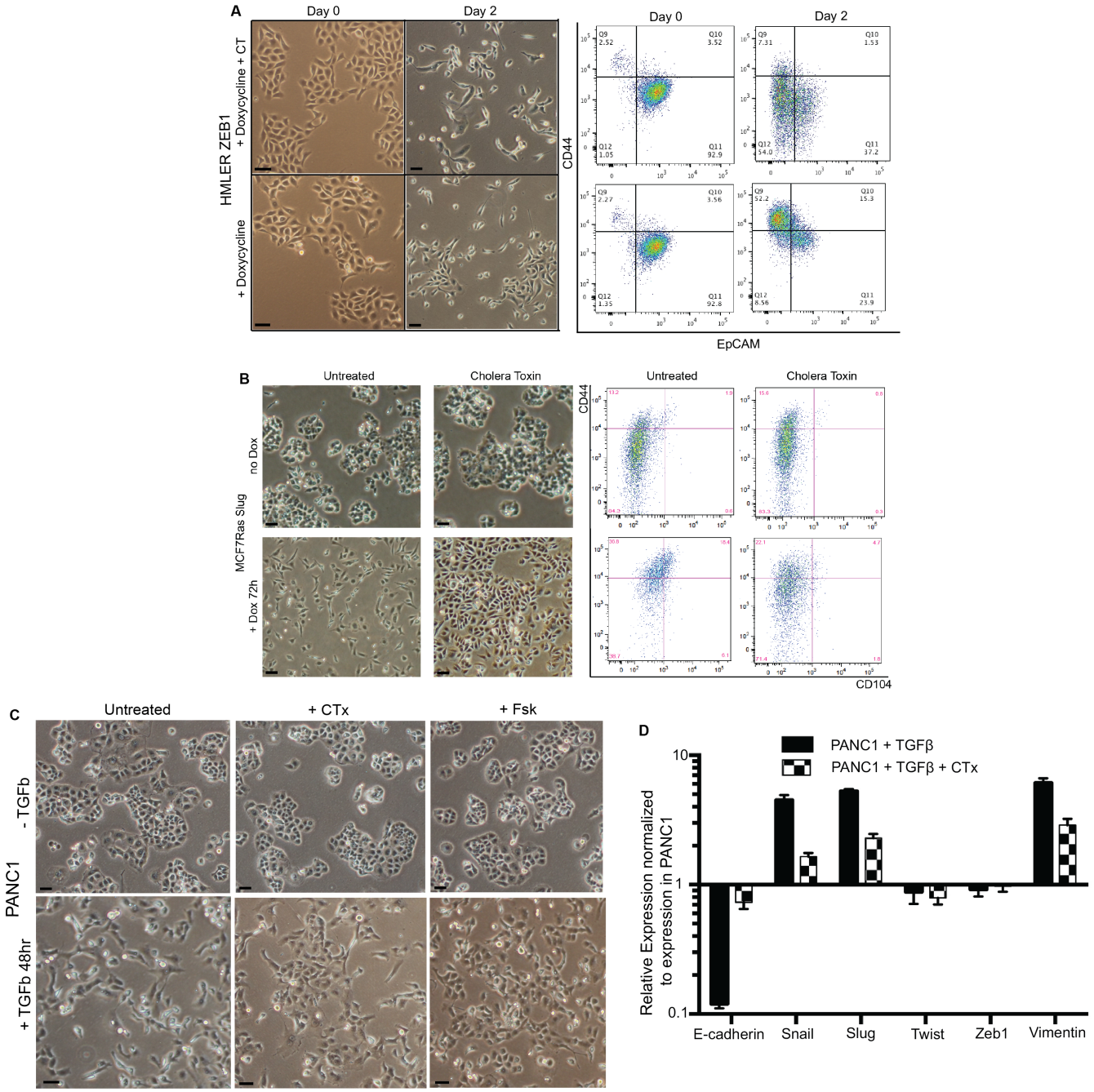

Figure S7: CTx-induced activation of PKA prevents the induction of an EMT. Addition of CTx delays the ability of HMLER-Zeb1 (A), MCF7Ras (B) and PANC1 cells (C) to undergo an EMT as observed by differences in morphology, expression of cell surface markers and qPCR of epithelial and mesenchymal markers. All scale bars - 25µm.

Supplementary Figure 8:

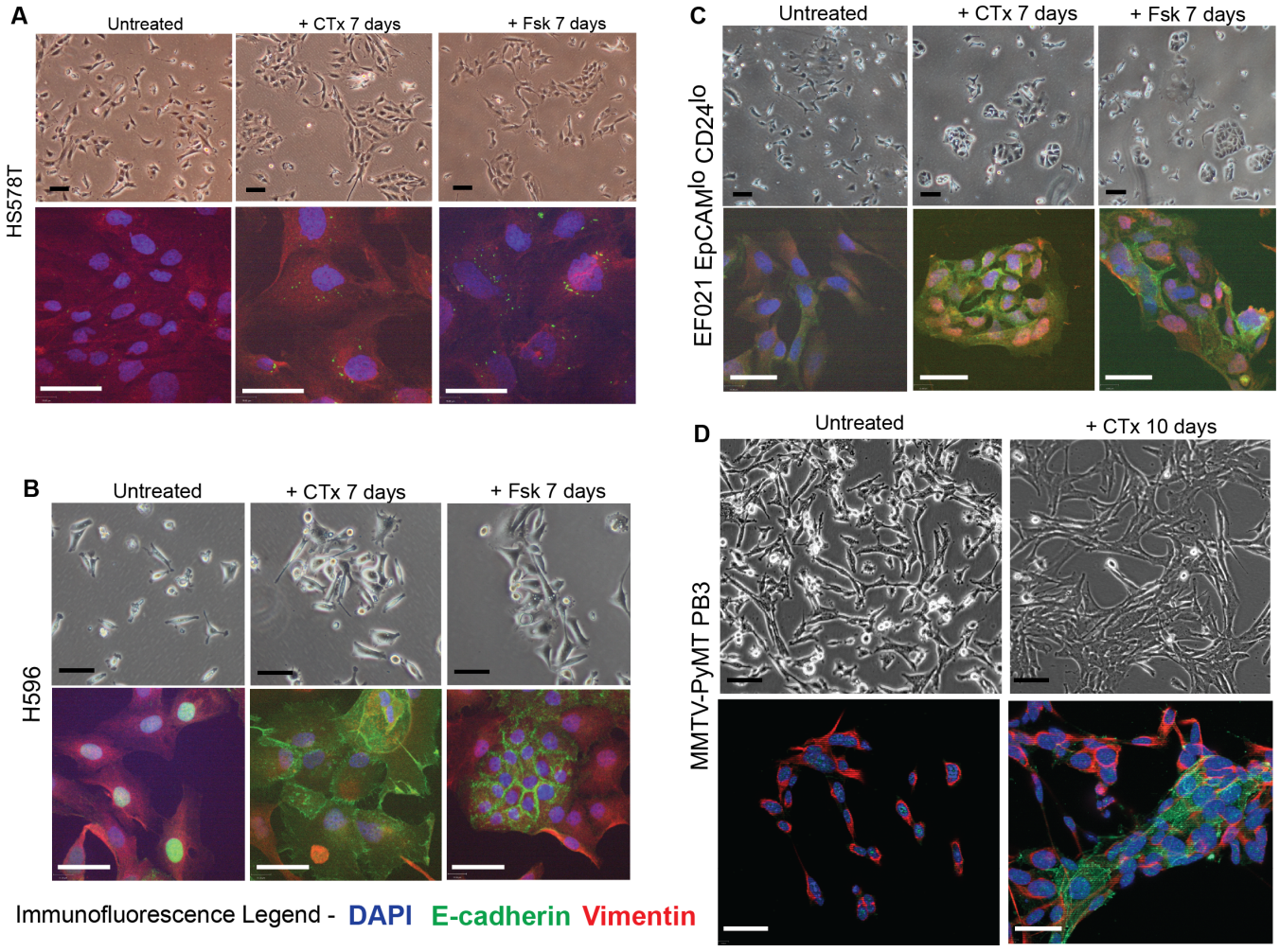

Figure S8: CTx-induced activation of PKA induces the acquisition of epithelial properties. CTx was able to induce epithelial properties in Hs578T (A), H596 (B), EF021 (C) and MMTV-PyMT PB3 cells (D). All scale bars - 25µm.

Supplementary Figure 9:

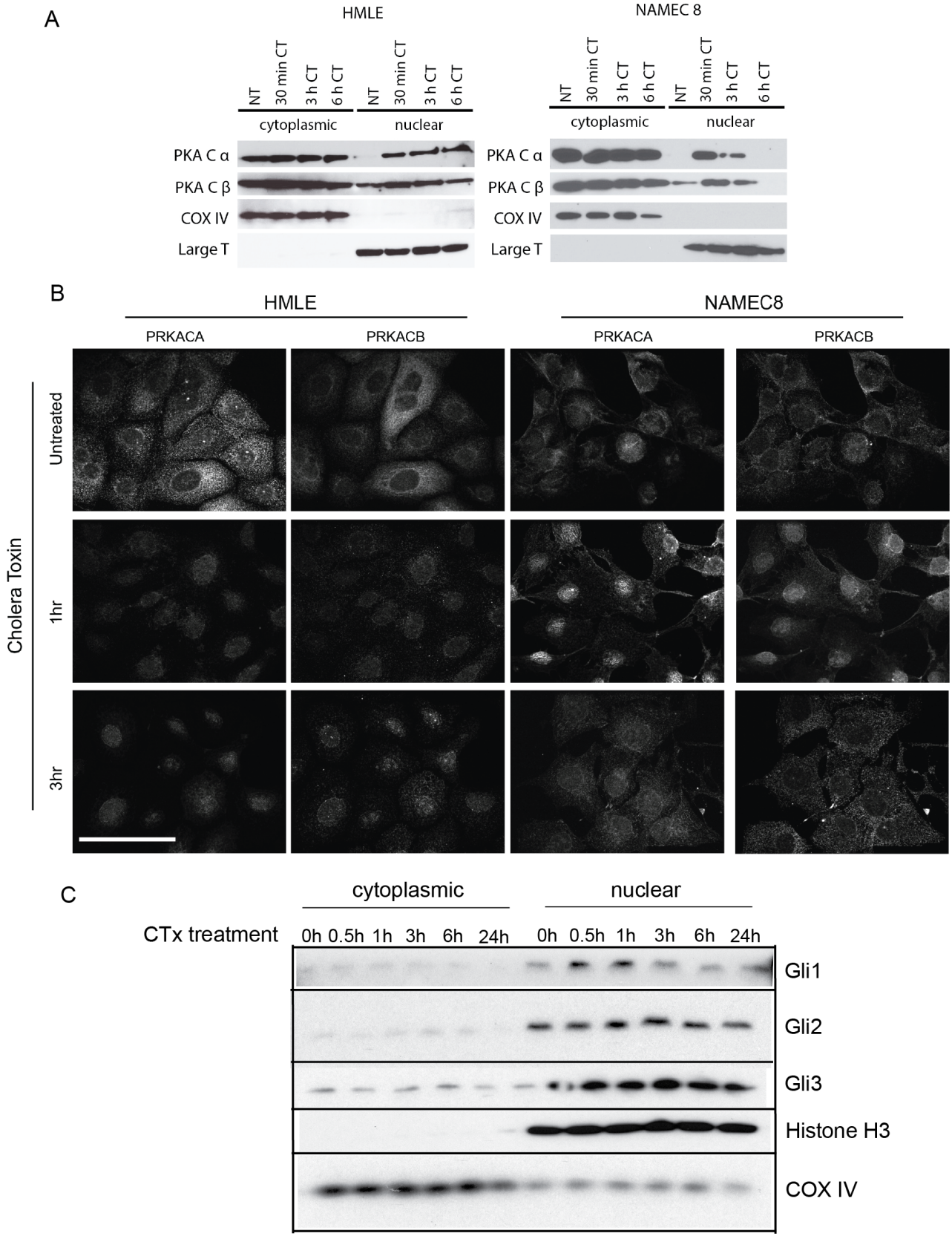

Figure S9: Dynamics of PKA and Gli translocation following activation with CTx. Within 30 minutes of treatment of the HMLE or N8 cells, nuclear translocation of PKA-Cα and PKA-Cβ was observed. Both proteins remain in the nucleus in HMLE cells for at least 6 hours, where in the N8 cells they leave the nucleus and return to the cytoplasm after 3 hours. Dynamics were assayed by (A) immunoblotting of nuclear and cytoplasmic fractionation of cell lysates and (B) immunofluorescence of cells. Similarly the translocation of the Gli1, Gli2 and Gli3 proteins were observed (C). All scale bars - 25μm.

Supplementary Figure 10:

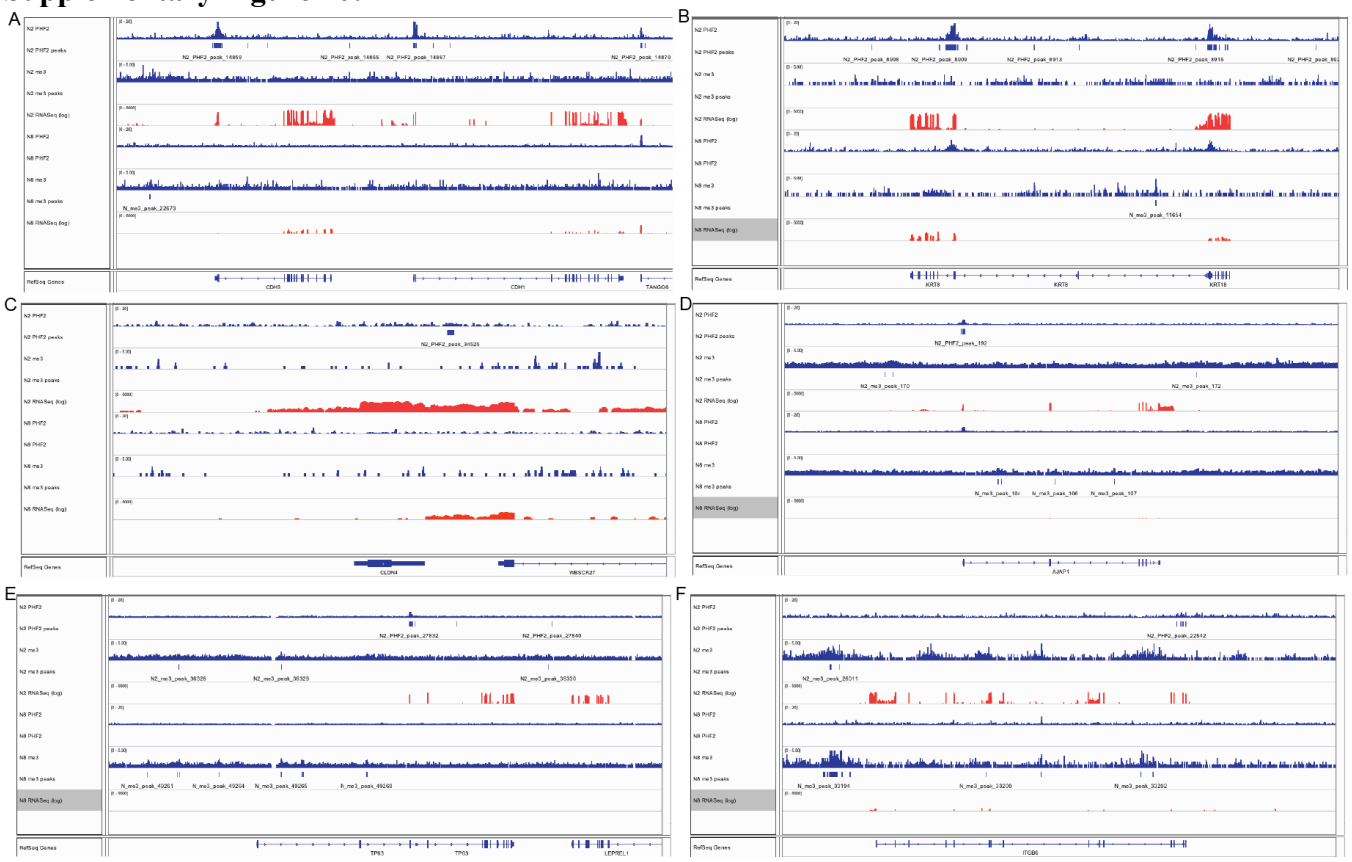

Figure S10: RNA-Seq and ChIP-Seq reveal epigenetic reprogramming following activation of PKA. ChIP-Seq results show localization of PHF2 to genomic regions of epithelial genes in N8-CTx, but not N8 cells, including CDH1 (A), CLDN4 (B), TP63 (C), KRT8 (D), AJAP1 (E) and ITGB6 (F).

Supplementary Figure 11:

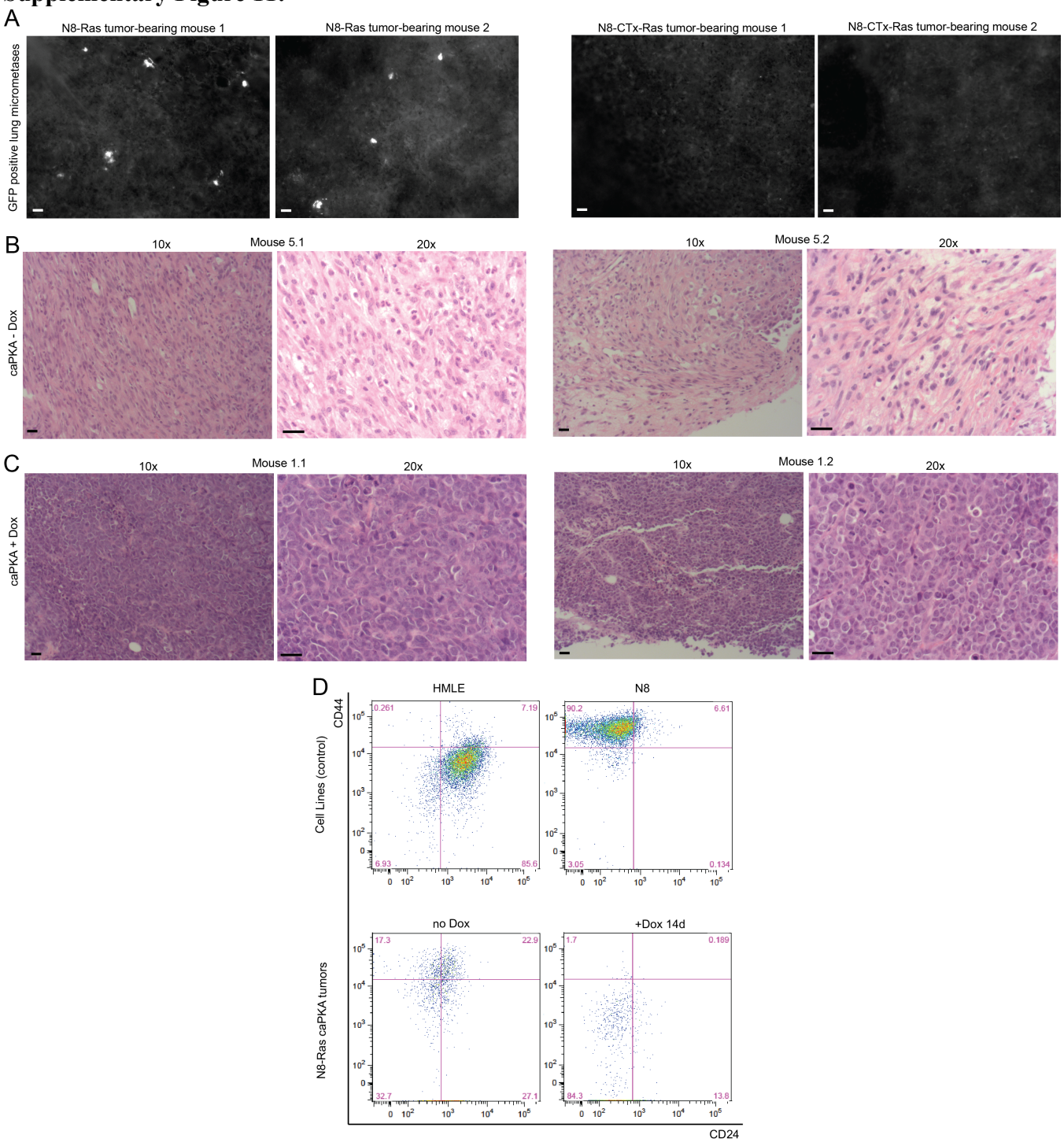

Figure S11: Activation of PKA in vivo leads to differentiation of tumors and a loss of ability to form lung micrometastases. Differentiation of N8-Ras tumors to a non-TIC state is accompanied by a loss of the ability to form micrometastases in the lung (A). N8-Ras cells form aggressive tumors that have a solid core. Tumor sections exhibit a sarcomatoid phenotype with very poor differentiation (B). Ectopic expression of PKA in vivo leads to the differentiation of these tumors, which become pasty and fluid-filled exhibiting a more differentiated epithelial morphology (C). This is accompanied by a loss of CD44 expression as observed in the lower FACS plots where tumors that originally expressed high levels of CD44, now have lost this expression after ectopic expression of caPKA (D). Cell surface CD44/24 expression levels of HMLE and N8 are presented on the top panel of this figure as a reference point. All scale bars - 25μm.

List of Supplementary Tables:

Table S1: List of genes differentially expressed between the HMLE and N8 cells as determined by RNA-Seq

Table S2: List of genes differentially expressed between N8 and N8-CTx cells as determined by RNA-Seq.

Table S3: List of genomic regions that contain PHF2 and no H3K9me2/3 marks in N8-CTx but lack PHF2 occupancy in N8 cells, instead containing H3K9me2/3 repressive marks.

Table S4: List of genomic regions that contain H3K9me2/3 repressive marks in N8 cells that have been treated with CTx in the presence of PHF2 knockdown